THE JOURNAL OF PHYSICAL CHEMISTRY B

pubs.acs.org/JPCB

Article

Inclusion Complexation of Organic Micropollutants with β-Cyclodextrin

Máté Erdős, Remco Hartkamp, Thijs J. H. Vlugt, and Othonas A. Moultos*

Cite This: J. Phys. Chem. B 2020, 124, 1218−1228

Read Online

ACCESS | Metrics & More | Article Recommendations | Supporting Information

ABSTRACT: Recently, β-cyclodextrin (βCD)-based polymers with enhanced adsorption kinetics and high removal capacity of organic micropollutants (OMPs) and uptake rates have been synthesized and tested experimentally. Although the exact physical−chemical mechanisms via which these polymers capture the various types of OMPs are not yet fully understood, it is suggested that the inclusion complex formation of OMPs with βCD is very important. In this study, the inclusion complex formation of OMPs with βCD in an aqueous solution is investigated by using the well-established attach−pull−release method in force field-based molecular dynamics simulations. A representative set of OMPs is selected based on the measured occurrences in surface and ground waters and the directives published by the European Union. To characterize the formation of the inclusion complex, the binding free energies, enthalpies, and entropies are computed and compared to experimental values. It is shown that computations using the q4md-CD/GAFF/Bind3P force field combination yield binding free energies that are in reasonable agreement with the experimental results for all OMPs studied. The binding enthalpies are decomposed into the main contributing interaction types. It is shown that, for all studied OMPs, the van der Waals interactions are favorable for the inclusion complexion and the hydrogen bond formation of the guest with the solvent and βCD plays a crucial role in the binding mechanism. Our findings show that MD simulations can adequately describe the inclusion complex formation of βCD with OMPs, which is the first step toward understanding the underlying mechanisms via which the βCD-based polymers capture OMPs.

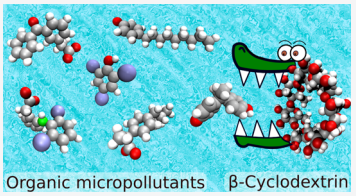

INTRODUCTION

Industrial, agricultural, and domestic activities give rise, directly or indirectly, to water contamination with a wide variety of harmful organic compounds.[1] Thousands of organic micropollutants (OMPs) of different origins and types, for example, industrial chemicals, pesticides, pharmaceuticals, personal-care products, human hormones, detergents, and their transformation products, are ubiquitously detected in surface and ground waters.[2−8] Despite their relatively low concentration, ranging from a few picograms to several micrograms per liter, many of those OMPs raise significant environmental and toxicological concerns.[9,10] Due to the large physicochemical diversity of OMPs and their low concentrations, conventional water and wastewater treatment processes (e.g., coagulation, flocculation, sedimentation, and sand filtration) achieve poor removal efficiency, essentially allowing many harmful OMPs to survive and find their way into the urban water cycle.[11−15] Several techniques for the efficient removal of OMPs have been developed, including oxidation, catalytic degradation, membrane filtration, and adsorption.[16−21] Adsorption-based technologies are considered promising due to their simplicity, low operational cost, and versatility through adsorbent selection. To this end, novel porous materials that can be tailor-designed have emerged as promising candidates for water treatment.[22,23]

Among the various families of porous materials (e.g., zeolites, silica, and activated carbons), porous polymer adsorbents exhibit distinct advantages, such as high surface areas, long-term physicochemical stability in water, low weights, mechanical flexibility, cost efficiency, good selectivity, fast adsorption kinetics, large capacity, and easy preparation and regeneration.[24−29] The numerous available molecular building blocks[27] of porous polymers allow for the synthesis of a wide variety of adsorbents having diverse structures and functions.

One promising building block is β-cyclodextrin (βCD), which is an inexpensive, nontoxic, naturally occurring cyclic oligosaccharide produced from starch.[30,31] Seven covalently connected glucose molecules form a truncated hollow cone-shaped molecule with a polar outer surface and a relatively nonpolar internal cavity. Due to this structure, βCD can form stable inclusion complexes with numerous compounds of appropriate size, shape, and polarity.[32−37] In recent years, βCD-based polymers with enhanced adsorption kinetics and high removal capacity of OMPs and uptake rates have been synthesized.[38−42] These polymers can capture a wide variety of OMPs, even at trace concentrations, via various mechanisms such as inclusion complexation, hydrogen bonding, and electrostatic and hydrophobic interactions.[42,43] As it is far from trivial to determine the contribution of each mechanism

Received: October 28, 2019
Revised: December 10, 2019
Published: January 24, 2020

https://dx.doi.org/10.1021/acs.jpcb.9b10122
J. Phys. Chem. B 2020, 124, 1218−1228

only based on experimental measurements, the exact physical chemistry via which the polymer captures the various types of OMPs (e.g., polar and nonpolar) is still not completely understood.[43] Previous studies have suggested that the inclusion complex formation of OMPs with the βCD building blocks of the polymer is one of the major mechanisms for capturing the OMP.[43]

Molecular simulation techniques can provide the necessary atomistic resolution to determine the effect of the various mechanisms contributing to the capture of OMPs.[44−46] In molecular simulations, the accurate representation of the interactions between atoms and molecules is provided by the force field and precise structural description of the polymer.[47,48] Currently, there is no readily available force field describing βCD-based polymers and their interactions with aqueous solvents and organic components. The derivation of such a force field requires an extensive number of experimental results and computationally intensive optimization scheme. As a first and computationally more attainable step toward understanding the capturing mechanisms, the interaction of the main building block of the polymer, βCD, in an aqueous solution with ions and guest molecules can be simulated using force fields from the literature. These simulations can be validated with reported experimental studies on the inclusion complexation of different guest molecules with βCD.

Computational studies testing various force field combinations for such systems have been reported recently.[49−51] Henriksen and Gilson[49] computed the binding free energies and binding enthalpies of 21 guest molecules with βCD using four different water models and two charge derivation methods and compared them with the available experiments. Molecules with three types of functional groups (i.e., ammoniums, alcohols, and carboxylates) attached to linear, aliphatic scaffolds and phenyl groups were studied. It was shown that the combination of the AM1-BCC/q4md-CD force field for the host, AM1-BCC/GAFF force field for the guest, and TIP3P for water produced the lowest deviation from experimental binding free energies, having a root mean square error (RMSE) = 3.35 kJ mol^{-1}. This force field combination, however, yielded a poor prediction of the binding enthalpy, deviating from experimental measurements by approximately a factor of 2. In the same study, significant variations in the computed free energies and enthalpies were obtained by using the q4md-CD (host), RESP/GAFF (guest), and different water force fields (i.e., TIP3P, TIP4Pew, and SPC).

Tang and Chang[50] reported computations of the binding free energy, binding enthalpy, and binding entropy of three aliphatic alcohols, methyl-butyrate, aspirin, 1-naphthyl-ethanol, and 2-naphthyl-ethanol with βCD. Two different force fields, that is, GAFF and q4md-CD, were used for the host (βCD), while the RESP/GAFF force field was used for the guest and the TIP3P for water. It was shown that the calculated binding free energies are in a reasonable quantitative agreement with the respective experiments, having an RMSE = 1.5−1.6 kcal mol^{-1}. Based on these results, it is evident that no available force field combination is able to reproduce both the experimental binding free energies and binding enthalpies within the error of the experimental measurements for a wide variety of molecule types. More discussion on the inclusion complexation of CDs with guest molecules for food, pharmaceutical, and separation technology applications can be found in the relevant literature, for example, guest molecules: anthracene,[52] isoflavones,[53−55] octyl glycoside,[56] ionic liquids,[57] chalcone,[58] and glycyrrhizic acid.[59] Some studies focus on the investigation of inclusion complex formation of widely used drug molecules (e.g. ketoprofen,[60,61] ibuprofen,[60,62,63] lidocaine,[64] and naproxen[60]) with βCD. To the best of our knowledge, there is no comprehensive study on the inclusion complex formation of OMPs with βCD, although this mechanism is one of the most important for the capturing capability of βCD polymers.[39,43]

In this study, a representative set of OMPs is selected based on the measured occurrences of the compound in surface and ground waters[6,8] and the directives by the European Union (EU).[65,66] The priority substance list, that is, directives 2000/60/EC and 2008/105/EC, which contains substances presenting a significant risk to the environment,[65] and the surface water watch list, which contains substances posing possible health risks,[66] were considered. The selected compounds are listed in Figure 1a. Bisphenol A (BPA) is an

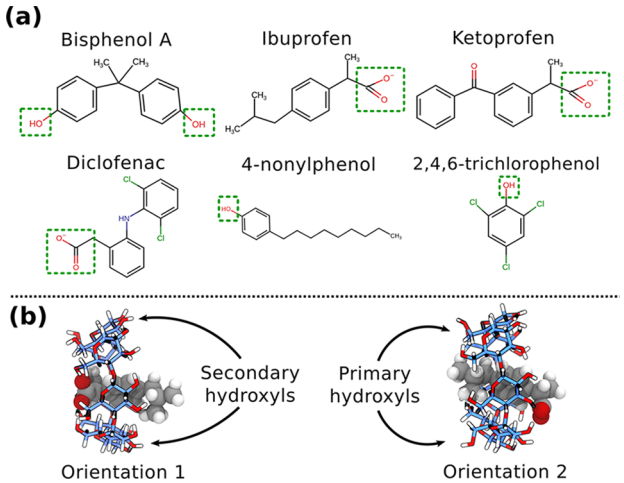

Figure 1. (a) Organic micopollutants (OMPs) studied in this work and (b) schematic illustrations of the different binding orientations. The main functional group of each molecule is indicated by a green rectangle. The orientations are defined based on the position of the main functional group. Orientation 1 refers to the binding orientation in which the main functional group of the molecule is near the primary hydroxyl groups of cyclodextrin. Orientation 2 refers to the binding orientation in which the main functional group of the molecule is near the secondary hydroxyl groups of cyclodextrin.

endocrine disruptor frequently detected in waters. Due to BPA's potential risk for public health, it also appears on the priority substance list published by the EU.[66] Diclofenac is a nonsteroidal anti-inflammatory drug that is listed as an emerging contaminant by the EU watch list.[66] 4-Nonylphenol (NP) is an endocrine disruptor that is detected at high concentrations in the aquatic environment and listed on the priority substance list published by the EU.[66] 2,4,6-Trichlorophenol (TCP) is a compound used as a pesticide and wood preservative. TCP is frequently detected in the aquatic environment and listed as a carcinogen.[67] Ibuprofen and ketoprofen are nonsteroidal anti-inflammatory drugs that are frequently detected in surface and ground waters[6,8] due to their widespread use.

The purpose of this work is to provide the necessary physical insight into the inclusion complexation of βCD with OMPs by performing MD simulations with the well-established attach−pull−release method of Henriksen et al.[68] To characterize the

https://dx.doi.org/10.1021/acs.jpcb.9b10122
J. Phys. Chem. B 2020, 124, 1218−1228

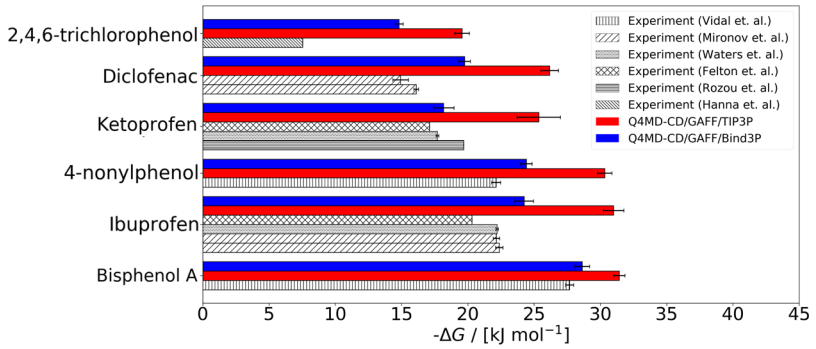

Figure 2. Computed and experimentally measured binding free energies of bisphenol A, ibuprofen, 4-nonylphenol, ketoprofen, diclofenac, and 2,4,6-trichlorophenol (TCP) molecules with βCD. The columns in red and blue represent the calculated binding free energies using the q4md-CD/GAFF/TIP3P[70,71,73] and q4md-CD/GAFF/Bind3P[50,70,71] force field combinations, respectively. The columns with the black-and-white patterns represent the experimental data, which is taken from the following sources: Pellegrino Vidal et al.,[88] Mironov et al.,[89] Waters et al.,[83] Felton et al.,[60] Rozou et al.,[84] and Hanna et al.[93]

inclusion complex formation, the binding free energy, binding enthalpy, and the average number of hydrogen bonds between βCD, OMPs, and water are calculated. The binding enthalpy is further decomposed into several contributions, that is, intramolecular, Lennard-Jones, and electrostatic. The choice of force fields used in this study was based on the work by Henriksen and Gilson[49] and Yin et al.[51] where the inclusion complexation of βCD with a wide and diverse range of guest molecules has been studied. The obtained binding free energies for all studied OMPs are in reasonable agreement with the experimental results. Two different binding orientations, shown in Figure 1b, are discussed. It is shown that, based on the obtained results, the contributions of the different interactions can be established and differences in binding strength can be explained. The remainder of this article is structured as follows. In the Simulation Methodology and Computational Details, the details about the calculation of the binding free energy and enthalpy are explained. In the Results and Discussion, the results of the binding free energy, enthalpy, and entropy calculations are presented and discussed for all OMPs.

SIMULATION METHODOLOGY AND COMPUTATIONAL DETAILS

All simulations were carried out using the GROMACS2018.2 software package.[69] The bonded and nonbonded force field parameters of βCD, OMPs, and sodium and chloride were taken from the q4md-CD,[70] General AMBER (GAFF),[71] and Joung-Cheatham force fields,[72] respectively. For the representation of water, two models were used: TIP3P[73] and Bind3P.[51] Bind3P is a water force field developed recently by Yin et al. who refitted the Lennard-Jones size and energy parameters of the TIP3P force field to better match the experimental host−guest binding data.[51] In this study, the Bind3P water model is used because it is specifically fitted to reproduce experimental host−guest data. Simulations with the TIP3P water model are also performed since this model is widely used along with GAFF. The partial charges of βCD, water, sodium, and chloride are taken from the original publications.[51,70,72,73] The partial charges for all OMPs were computed with restrained electrostatic potential (RESP) at the 6-31G* level of theory using the R.E.D. III.52 script[74] with the Gaussian09 RevB.01 software package.[75] GROMACS parameter files containing all force field parameters are provided in the Supporting Information. The nonbonded interactions were truncated at 9.0 Å, and analytic tail corrections are applied in the computation of the energies and pressures. The long-range electrostatic interactions are taken into account by using the particle-mesh Ewald (PME) method.[76] The stochastic leap-frog algorithm is used to integrate the equation of motion with a timestep of 2 fs. The scheme followed in all simulations is as follows: Initially, the energy of the system is minimized using the steepest descent method. Consequently, equilibration runs were performed for (i) 50 ps in the *NVT* ensemble at a temperature of 50 K, (ii) 1 ns in the *NVT* ensemble with a temperature ramping from 50 to 300 K, and (iii) 2 ns in the *NPT* ensemble at 300 K and 1 bar. The production runs were carried out in the *NPT* ensemble at the same temperature and pressure, regulated using the Langevin thermostat[77] and Berendsen barostat.[78]

To calculate the binding free energy of the selected OMPs with βCD, the attach−pull−release (APR) method[68] was used. A detailed description of the APR method can be found in the study reported by Henriksen et al.[68] The binding enthalpy of the OMPs with βCD was calculated with the solvent-balance method.[79] The errors in the binding free energies are calculated using the built-in GROMACS tools.[69] The errors in the binding enthalpies are calculated with the block average method.[80] The details on the implementation of the APR and the solvent-balance method are reported in the Supporting Information.

It is important to note that several orientations of the OMPs can contribute to the binding free energy and enthalpy with βCD.[49,68] In experiments, these binding orientations occur naturally, and therefore the measurements of the binding free energies and enthalpies do not explicitly distinguish between them. In this study, the combined binding free energies and enthalpies for two different binding orientations are calculated for all OMPs. The orientations are shown in Figure 1b. The approach for calculating the combined binding free energies and enthalpies is presented in the Supporting Information. In experimental studies, the binding constant, K_a, or the dissociation constant, $K_d = 1/K_a$, of the host−guest complex is reported. The binding constant is a special type of equilibrium constant, which is related to the concentration of the complex, free host, and free guest in the solution.[81] To compare experimental and simulation results, the binding free energy of the guest can be calculated from the binding/dissociation constant using:[82]

https://dx.doi.org/10.1021/acs.jpcb.9b10122
J. Phys. Chem. B 2020, 124, 1218−1228

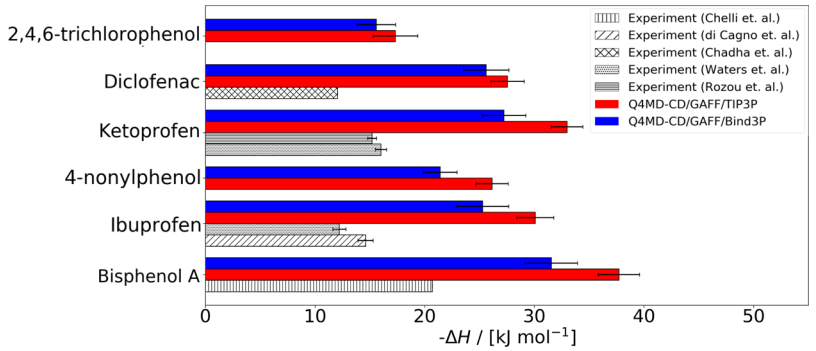

Figure 3. Computed and experimentally measured binding enthalpies of bisphenol A, ibuprofen, 4-nonylphenol, ketoprofen, diclofenac, and 2,4,6-trichlorophenol (TCP) molecules with βCD. The columns in red and blue represent the calculated binding enthalpies using the q4md-CD/GAFF/TIP3P[70,71,73] and q4md-CD/GAFF/Bind3P[51,70,71] force field combinations, respectively. The columns with black-and-white patterns represent the experimental data, which is taken from the following sources: Chelli et al.,[90] di Cagno et al.,[91] Chadha et al.,[92] Waters et al.,[83] and Rozou et al.[84]

$$\Delta G_{\text{combined}} = RT \ln \frac{K_d}{C^\circ} \quad (1)$$

where $\Delta G_{\text{combined}}$ is the combined free energy of the different orientations, R is the universal gas constant, T is the temperature, and C° is the standard reference concentration (C° = 1 M).

RESULTS AND DISCUSSION

Binding Free Energy. In Figure 2, the experimentally measured and computed binding free energies of the OMPs with βCD using the q4md-CD/GAFF/TIP3P and q4md-CD/GAFF/Bind3P force field combinations are shown. It can be observed that the experimentally measured binding free energies for specific OMPs vary between studies. This may be due to the different experimental conditions or measurement techniques applied in the studies. In Figure 2, three sets of experimental results are presented for the binding free energy of ketoprofen with βCD. In the study reported by Waters et al.,[83] the binding free energy was measured by isothermal titration calorimetry (ITC). In the studies by Felton et al.[60] and Rozou et al.,[84] phase solubility measurements were performed. It can be seen that, despite using the same measurement technique, the reported binding free energies by Felton et al.[60] and Rozou et al.[84] differ by ∼2.5 kJ mol^{-1}. The most probable cause of this discrepancy is that, in the measurements of Felton et al.,[60] no buffer is applied to keep the pH of the solution constant, while in the study by Rozou et al.,[84] a phosphate buffer is applied. It has been shown that, due to the competition of the ions and guest molecules for the cavity, the type and concentration of the applied buffer affect the binding affinity of guest molecules with βCD[85,86] and other host molecules (e.g., curcurbit[7]uril and octa-acid).[87] The measurements by Waters et al.[60] and Rozou et al.[84] are in the same conditions (e.g., type of buffer and temperature) but using different measurement techniques. Thus, the discrepancy between the reported experimental studies may be attributed to the different techniques. To quantitatively compare the binding affinity of different guest molecules with βCD, experiments at the same conditions and using the same technique should be carried out. To the best of our knowledge, a systematic study reporting the experimentally measured binding free energies of all selected OMPs with βCD is lacking.

The binding free energy measurements by Pellegrino Vidal et al.[88] are shown in Figure 2. It can be seen that BPA forms a more stable complex with βCD than with NP ($\Delta G_{\text{binding}}$ is equal to −27.68 and −22.13 kJ mol^{-1}, respectively). Our calculations of the binding free energies predict the same trend of binding affinity for these molecules. Interestingly, the experimentally measured binding free energy of BPA with the βCD-based polymer reported by Alsbaiee et al.,[39] $\Delta G_{\text{binding}}$ = −27.26 kJ mol^{-1}, is very close to the calculated binding free energy of BPA with just the βCD using the Bind3P water model, $\Delta G_{\text{binding}}$ = −28.63 kJ mol^{-1}. Moreover, the computed value is almost identical with the experimentally reported binding free energy of BPA with βCD ($\Delta G_{\text{binding}}$ = −27.68 kJ mol^{-1}).[88] Mironov et al.[89] reported the binding free energy of diclofenac and ibuprofen, measured both by affinity capillary electrophoresis coupled with mass spectrometry (CE-MS) and with UV detection (CE-UV) techniques. Both experimental techniques predict that ibuprofen has a more negative binding free energy than that of diclofenac. This indicates that ibuprofen forms a more stable inclusion complex with βCD than that with diclofenac. The same trend is observed from the MD calculations using both water force fields. The experimental measurements by Felton et al.[60] and Waters et al.[83] for ketoprofen and ibuprofen are also shown also in Figure 2. In both studies, it was found that ibuprofen has a more negative binding free energy with βCD than that of ketoprofen, indicating that ibuprofen forms a more stable inclusion complex than that of ketoprofen. Our MD simulations are in line with these experimental findings. It is important to note here that, since the experiments are performed at different conditions and with varying techniques, an exact quantitative comparison of the computed and experimentally measured binding free energies cannot be carried out for the selected OMPs. From the qualitative point of view, the computed binding free energies using both TIP3P and Bind3P water force fields follow the trend of the experiments, that is, MD simulations can predict which OMPs form more stable inclusion complexes with βCD. The calculated binding free energies of all OMPs using the Bind3P water force field show a slight overestimation compared to the corresponding experimental values but are still in reasonable agreement, having an RMSE = 3.5 kJ mol^{-1}, which corresponds to a deviation of 24%. Consistent with the findings by Henriksen and Gilson,[49] our MD results for the binding free energies using the TIP3P water force field considerably overestimate the experimental measurements by approximately 59%.

Binding Enthalpy. The computed binding enthalpies of the OMPs with βCD are shown in Figure 3, along with the respective experimental results obtained from the litera-

https://dx.doi.org/10.1021/acs.jpcb.9b10122
J. Phys. Chem. B 2020, 124, 1218−1228

ture.[83,84,90−93] The available experimental binding enthalpies for the selected compounds are scarcer compared to binding free energies. Experimentally measured binding enthalpies for NP and TCP with βCD are not available in the literature. The only available binding enthalpies of ketoprofen and ibuprofen are from the study by Waters et al.[83] who performed measurements using ITC.[83] In Figure 3, both the experimental and MD results show that the binding of ketoprofen ($\Delta H^{\text{ketoprofen}}_{\text{Bind3P}} = -27.22$ kJ mol^{-1}, $\Delta H^{\text{ketoprofen}}_{\text{TIP3P}} = -32.98$ kJ mol^{-1}, and $\Delta H^{\text{ketoprofen}}_{\text{Experiment}} = -16.00$ kJ mol^{-1}) is more exothermic than the binding of ibuprofen ($\Delta H^{\text{ibuprofen}}_{\text{Bind3P}} = -25.28$ kJ mol^{-1}, $\Delta H^{\text{ibuprofen}}_{\text{TIP3P}} = -30.10$ kJ mol^{-1}, and $\Delta H^{\text{ibuprofen}}_{\text{Experiment}} = -14.60$ kJ mol^{-1}). Similar to the binding free energy results, the computed binding enthalpies follow the trend of the experimental measurements, which is $\Delta H^{\text{BisphenolA}} < \Delta H^{\text{Ketoprofen}} < \Delta H^{\text{Diclofenac}} \approx \Delta H^{\text{Ibuprofen}} < \Delta H^{4-\text{Nonylphenol}} < \Delta H^{2,4,6-\text{Trichlorophenol}}$. As can be seen in Figure 3, the computed binding enthalpies using the Bind3P water force field are systematically closer to the experimental values compared to simulations using TIP3P. This finding is in agreement with Yin et al.[51] who performed binding free energy and enthalpy computations using TIP3P and Bind3P force fields for 21 βCD−guest pairs. Based on our comparison of the experimental and computed binding free energies and enthalpies, it can be concluded that MD simulation techniques have the potential to predict the binding affinity of OMPs with βCD. The quantitative predictive power of the method is expected to improve even more with the development of improved force fields, which can be developed considering also the binding thermodynamics data.[49]

To obtain a better understanding of the binding mechanism, the contributions of different interactions are investigated. The binding enthalpy is decomposed to three contributions: (1) intramolecular (bonded, 1-4 LJ, and 1-4 electrostatic terms), (2) Lennard-Jones, and (3) electrostatic interactions. In Figure 4, the decomposition of the computed enthalpies using the Bind3P water force field is shown for all studied OMPs. Computations considering both binding orientations are shown (representations of the two orientations are shown in Figure 1b). As can be seen in Figure 4, for all OMPs studied and both binding orientations, the Lennard-Jones and electrostatic contributions are negative, which means that these interactions are favorable for the inclusion complex formation. The binding is hindered by intramolecular interactions (positive energy) for almost all OMPs, except for ketoprofen. The main opposing terms in the intramolecular contribution are the 1-4 interactions, which mainly originate from the conformational change of the host upon binding (Table S1). For the case of orientation 1 of ketoprofen, the 1-4 electrostatic term becomes favorable and results in a negative intramolecular contribution to the binding (Table S1).

To further investigate the role of the different intramolecular contributions, the position of the carboxyl oxygens relative to the primary and secondary rims of βCD is investigated for both orientations of ibuprofen and ketoprofen (Figure 5). In Figure 5c−f, the distances of the carboxylic oxygens from the center of mass of the primary or secondary oxygens of βCD are shown for both orientations of ibuprofen and ketoprofen. In orientation 1, the carboxyl group of ketoprofen shows a preference for tighter binding to the primary rim of βCD than that of ibuprofen (Figure 5c). The tighter binding of the carboxyl oxygen at the narrower rim provides the possibility for the oxo group to form hydrogen bonds with the oxygen atoms

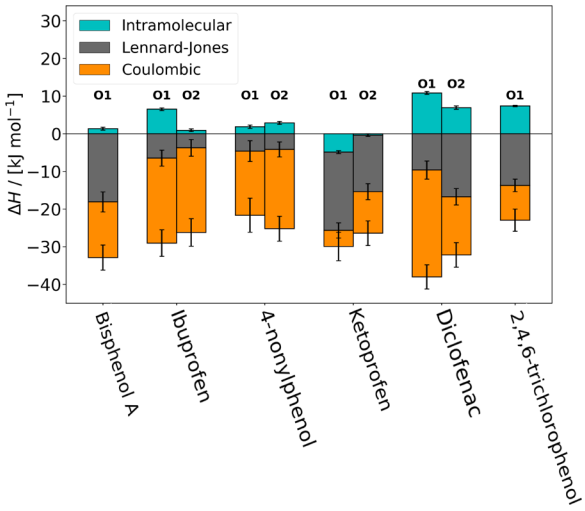

Figure 4. Computed enthalpy decomposition of the binding orientations for bisphenol A, ibuprofen, 4-nonylphenol, ketoprofen, diclofenac, and 2,4,6-trichlorophenol (TCP) molecules with βCD. The O1 and O2 labels indicate orientations 1 and 2, respectively. The intramolecular (bonded, 1-4 LJ, and 1-4 Coulombic terms) contribution is shown in cyan, the Lennard-Jones contribution in gray, and the electrostatic contribution in orange. The bars representing the contributions of the different interaction types are stacked on each other.

at the wider rim of βCD (see Figure 5c,d). In orientation 2, the carboxyl oxygen of ketoprofen shows a slight preference compared to ibuprofen toward the solvent, which brings the oxo group closer to the oxygens of the wider rim of βCD (Figure 5e,f). The binding configuration of ketoprofen results in favorable host configurations most probably due to the stabilizing effects of the hydrogen bonds between the host and guest molecules. The stabilizing effects of the hydrogen bonds formed between ketoprofen and βCD are also discussed in the study reported by Guzzo et al.[61] In that study, the inclusion complexation of ketoprofen with βCD is investigated both by performing nuclear magnetic resonance (NMR) measurements and MD simulations.

Although the contributions from Lennard-Jones and electrostatic interactions are favorable for the binding of all studied guest molecules, the relative magnitude of the two contributions can differ regardless of the polarity or the protonation state of the OMP. The binding enthalpy can be decomposed into two terms, namely, the host−guest and desolvation. The host−guest term accounts for the intermolecular host−guest interactions and for the change of enthalpy due to conformational changes of the host and guest upon binding. The desolvation term represents the effects due to the binding of the guest molecule. This term comprises the interaction change between host and water, guest and water, and water and water upon binding. In Figure 6, the decomposed enthalpies into the host−guest and desolvation terms for orientations 1 and 2 are shown for all studied OMPs. Since all desolvation terms are positive (i.e, inclusion complexation is hindered) and all host−guest terms are negative (inclusion complexation is favored), the negative value of the desolvation term ($-\Delta H_{\text{desolvation}}$) is shown in Figure 6 to make the comparison to the host−guest term more representative. For orientation 1, the LJ interactions are the dominant contribution to the host−guest term for all OMPs except for ketoprofen. The LJ contribution scales with the number of

https://dx.doi.org/10.1021/acs.jpcb.9b10122
J. Phys. Chem. B 2020, 124, 1218−1228

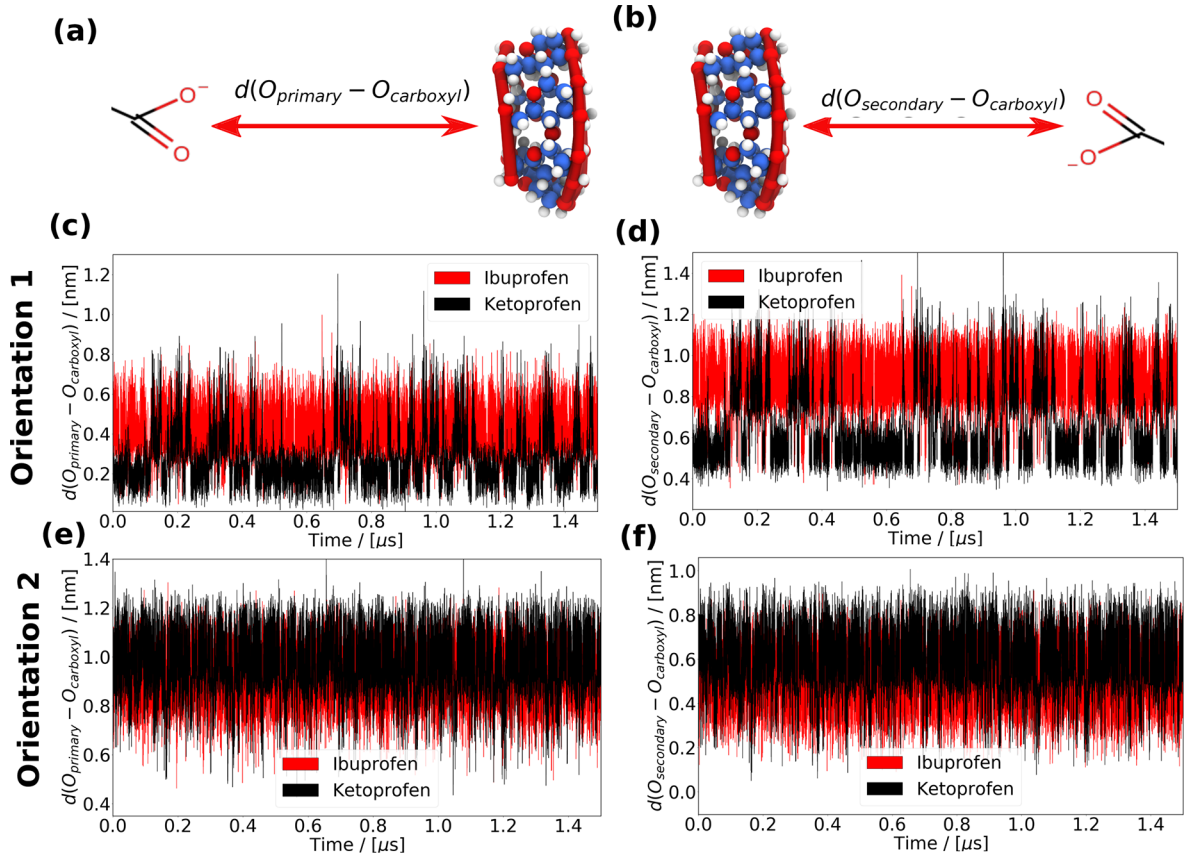

Figure 5. Distance of the carboxylic oxygens from the center of mass of the primary or secondary hydroxyl groups of βCD for both orientations of ketoprofen and ibuprofen. (a, b) The schematic representations of the distances of the carboxylic oxygens from the center of mass of the primary and secondary hydroxyl groups are shown, respectively. (c, d) The distances between the carboxylic oxygens and the center of mass of the primary and secondary hydroxyl groups are shown for orientation 1, respectively. (e, f) The distances between the carboxylic oxygens and the center of mass of the primary and secondary hydroxyl groups are shown for orientation 2, respectively.

atoms contributing to the formation of the inclusion complex. By comparing the LJ contributions of the two orientations, it can be seen that the LJ terms are slightly larger for orientation 1. This difference can be attributed to the stronger interactions of the OMPs with the atoms in the narrow rim of βCD. In Figure 6, it can be observed that the electrostatic interactions become dominant in the host−guest term for both orientations of ketoprofen and for orientation 2 of diclofenac and ibuprofen. The major role of the electrostatic interactions in the host−guest term is caused by the hydrogen bond formation of the OMPs with βCD as it will be discussed in the following paragraph.

In Figure 6, it can be observed that both LJ and electrostatic contributions of the desolvation term show the same trend as the host−guest term. Orientation 1 has a larger LJ contribution to the desolvation term than that of orientation 2. This means that more atoms are involved in the complex formation and lose interactions with water upon binding in orientation 1.

Hydrogen Bonding. In Figure 7, the number of hydrogen bonds between the solvent−guest and host−guest molecules is shown. From Figure 7, it can be observed that the guest loses hydrogen bonds with the solvent upon binding to βCD. For example, ibuprofen (in orientation 2) loses ∼2 hydrogen bonds with the solvent upon binding to βCD. The host also loses interactions with the solvent upon binding of the guest molecule. The free host forms approximately 33 hydrogen bonds with the solvent. The host may lose some of these hydrogen bonds upon forming an inclusion complex with an OMP. For example, βCD loses approximately three of these hydrogen bonds in the binding with ketoprofen in orientation 1. All data on hydrogen bonding are listed in Table S3 in the Supporting Information. The loss of these hydrogen bonds plays a dominant role in determining the magnitude of the electrostatic contribution of the desolvation term. The more hydrogen bonds are lost between the host, guest, and solvent, the greater the electrostatic contribution in the desolvation term. The net change in the number of hydrogen bonds upon binding of the OMP is shown in Table S3 in the Supporting Information. As can be seen in Figure 7, BPA, NP, and TCP molecules practically do not form hydrogen bonds with βCD (orange part of the bars). The absence of hydrogen bonds results in considerably lower electrostatic contributions to the host−guest and desolvation terms, as discussed earlier and can be explicitly seen in Figure 6. Ibuprofen and diclofenac form fewer hydrogen bonds in orientation 1 than in orientation 2. In orientation 2, the OMPs can form more hydrogen bonds with βCD due to the more accessible OH groups and less steric hindrance, which can lead to a more stable inclusion complex. Due to the positions of the oxo and carboxyl groups in the ketoprofen molecule, they can form almost the same amount of hydrogen bonds in both binding orientations. This indicates that the dominant electrostatic contribution in the host−guest term (see Figure 6) is caused by the hydrogen bond formation between the guest and host molecules.

https://dx.doi.org/10.1021/acs.jpcb.9b10122
J. Phys. Chem. B 2020, 124, 1218−1228

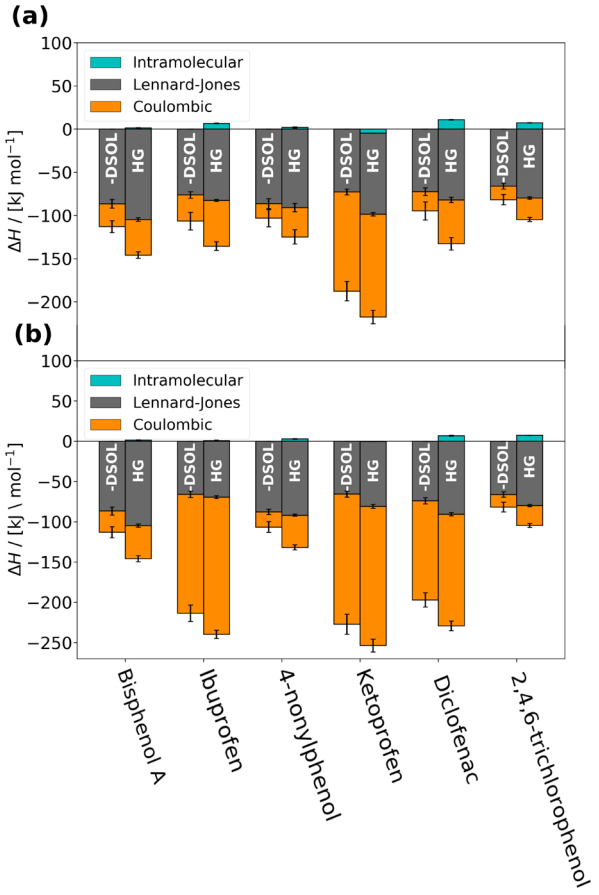

Figure 6. Contributions of the host−guest interactions and desolvation effects to the binding enthalpy for (a) orientation 1 and (b) orientation 2 of all studied OMPs. Since the host−guest and desolvation terms have opposite signs, the negative value of the desolvation term ($-\Delta H_{desolvation}$) is shown. The intramolecular (bonded, 1-4 LJ, and 1-4 Coulombic terms) contribution is shown in cyan, the Lennard-Jones contribution in gray, and the electrostatic contribution in orange. The bars representing the contributions of the different interaction types are stacked on each other. The -DSOL and HG labels indicate the desolvation and host−guest terms, respectively.

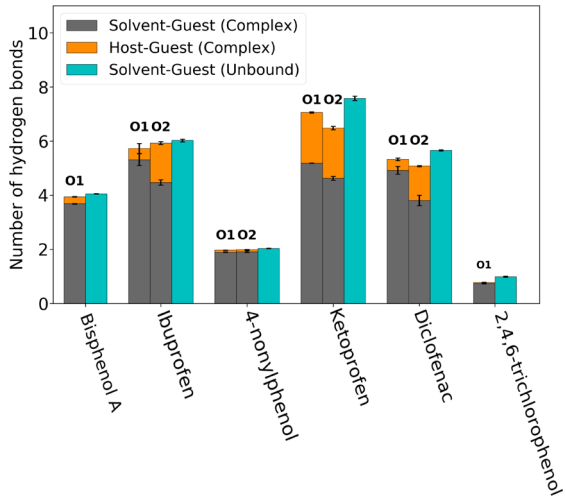

Figure 7. Average number of hydrogen bonds formed between the solvent and free guest (cyan), host and guest (orange), and solvent and guest in the inclusion complex (gray). The bars representing the number of hydrogen bonds between the different molecule types are stacked on each other. The O1 and O2 labels indicate orientations 1 and 2, respectively.

In the study reported by Brown et al.,[94] experimental measurements of the inclusion complex formation of ibuprofen with permethylated βCD (PMβCD) were reported. It was found that, in the stable inclusion complex, the isobutyl group of ibuprofen lies in the cavity. The carboxyl group forms a hydrogen bond with the methoxy group of the wider rim (orientation 2), which evidently contributes to the stability of the inclusion complex. This finding is in line with our simulation results, which show that the binding of ibuprofen in orientation 2 is more stable than in orientation 1 (see Table S2 in the Supporting Information). Brown et al.[94] also reports detailed structural properties of the ibuprofen−PMβCD inclusion complex; some of which are comparable with our simulation results. The radius of the heptagon, which is the distance of the O4 oxygens from the center of mass of the seven O4 atoms in the CD (see Figure S1a in the Supporting Information), is 4.99 Å in PMβCD and on average 4.93 ± 0.3 Å in our simulations. This shows that the cavity size of the CDs in the experiment and simulations is equal within the uncertainties of the computation. The glycosidic oxygen angle, which is the angle between the O4 oxygens of the residues of the CDs (see Figure S1b in the Supporting Information), is found to be 127.4° for PMβCD and 127.15 ± 1.64° in our simulations. The agreement in the glycosidic oxygen angles suggests that the shape of the host cavity is not influenced by the functionalization of βCD. The number of intramolecular hydrogen bonds in the experiments of PMβCD is found to be seven. In our simulation, βCD forms approximately six intramolecular hydrogen bonds. These findings suggest that the configuration of βCD and PMβCD is similar in the inclusion complex with ibuprofen.

Braga et al.[95] performed measurements to investigate the 1:2 ibuprofen−βCD inclusion complex. The two βCDs in the complex are linked by the formation of hydrogen bonds between the secondary hydroxyl groups of the wider rim. Braga et al.[95] found that, in the stable 1:2 inclusion complex, the carboxyl group of the ibuprofen protrudes from the smaller rim of βCD. In our study on the 1:1 inclusion complex, this configuration of ibuprofen can be identified as orientation 1, and our findings indicate that this orientation is less stable compared to orientation 2. This disagreement with the experiments can be most probably attributed to the fact that ibuprofen in the 1:2 complex cannot form hydrogen bonds with the wider rims of βCD. This shows clearly that the dimerization of βCD has a significant effect on the configuration of the inclusion complex.

Binding Entropy. The binding entropy can be computed by subtracting the calculated binding free energy from the binding enthalpy: $\Delta G = \Delta H - T\Delta S$. The computed binding entropies for all studied OMPs and both orientations are shown in Figure 8. Due to the subtraction between very big numbers, the error propagation results in considerable errors for the binding entropy (σ = 1.9−3.4 kJ mo1^{-1}). From Figure 8, it can be observed that the binding entropies for orientation 2 are smaller than for orientation 1, indicating that orientation 2 is entropically more favorable for binding. This difference can be possibly explained by the tighter binding of OMPs in orientation 1, which results in a less flexible βCD. The tighter binding of OMPs is also indicated by the more favorable (i.e., more negative) Lennard-Jones contributions of the host−guest term in orientation 1 than in orientation 2 as can be seen in

https://dx.doi.org/10.1021/acs.jpcb.9b10122
J. Phys. Chem. B 2020, 124, 1218−1228

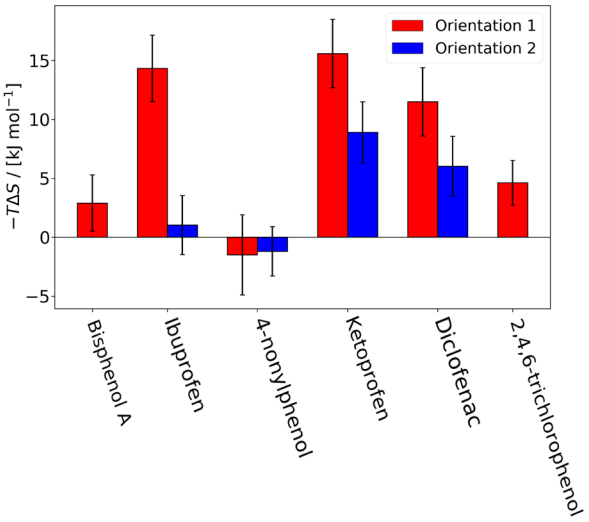

Figure 8. Computed binding entropy for orientation 1 (red) and orientation 2 (blue) for all OMPs studied.

Figure 6. This is caused by fewer atoms participating in the inclusion complex formation.

CONCLUSIONS

In this work, the binding free energy and enthalpy of bisphenol A, ibuprofen, ketoprofen, diclofenac, 4-nonylphenol, and 2,4,6-trichlorophenol with βCD are computed by performing force-field-based MD simulations. The computed binding free energies using the Bind3P water force field are in reasonable agreement with the available experimental results. The deviations between the computed and experimentally measured binding enthalpies are found to be considerable. This is in agreement with the findings of Henriksen and Gilson.[49] The computed binding enthalpies follow the trend of the experimental measurements. To obtain a better understanding of the binding mechanism, the effect of the intramolecular, van der Waals, and electrostatic interactions on the inclusion complex formation is investigated by the decomposition of the binding enthalpy. It is shown that, for all studied OMPs, the van der Waals and electrostatic interactions are favorable for the inclusion complex formation, but the relative magnitude of the two contributions can differ regardless of the polarity or protonation state of the OMP. To reveal the effect of the different interactions, the binding enthalpy is decomposed into host−guest and desolvation terms. It is observed that the magnitude of the contribution from the van der Waals interactions depends on the number of atoms participating in the complex formation. It is shown that the hydrogen bond formation of the guest with the solvent and βCD plays a crucial role in the binding mechanism. Our findings show that MD simulations using the APR method[68] can provide important physical insight into the inclusion complex formation of βCD with OMPs. Inclusion complexation is suggested to be one of the main mechanisms via which βCD-based polymers capture OMPs; thus, our findings can be used for the design and optimization of these materials.

ASSOCIATED CONTENT

Supporting Information

The Supporting Information is available free of charge at https://pubs.acs.org/doi/10.1021/acs.jpcb.9b10122.

Computational details about the binding free energy and enthalpy calculations (PDF)

Parameter files in GROMACS format for all OMPs and βCD (ZIP)

Tables S1-S3: Enthalpy decomposition for all OMPs for orientations 1 and 2, summary of the calculated binding free energies, enthalpies, and entropies for all OMPs with orientations 1 and 2 using the TIP3P and Bind3P water models, and the number of hydrogen bonds formed between the host−guest, guest−solvent, and host−solvent in the bound and unbound state (XLS)

AUTHOR INFORMATION

Corresponding Author

Othonas A. Moultos − *Engineering Thermodynamics, Process & Energy Department, Faculty of Mechanical, Maritime and Materials Engineering, Delft University of Technology 2628CB Delft, Netherlands;* orcid.org/0000-0001-7477-9684; Email: o.moultos@tudelft.nl

Authors

Máté Erdős − *Engineering Thermodynamics, Process & Energy Department, Faculty of Mechanical, Maritime and Materials Engineering, Delft University of Technology 2628CB Delft, Netherlands*

Remco Hartkamp − *Engineering Thermodynamics, Process & Energy Department, Faculty of Mechanical, Maritime and Materials Engineering, Delft University of Technology 2628CB Delft, Netherlands;* orcid.org/0000-0001-8746-8244

Thijs J. H. Vlugt − *Engineering Thermodynamics, Process & Energy Department, Faculty of Mechanical, Maritime and Materials Engineering, Delft University of Technology 2628CB Delft, Netherlands;* orcid.org/0000-0003-3059-8712

Complete contact information is available at: https://pubs.acs.org/10.1021/acs.jpcb.9b10122

Notes

The authors declare no competing financial interest.

ACKNOWLEDGMENTS

The authors are very thankful to Michael K. Gilson, Niel Henriksen, and David Slochower for helping in the correct implementation of the attach−pull−release method. This work was sponsored by NWO Exacte Wetenschappen (Physical Sciences) for the use of supercomputer facilities with financial support from the Nederlandse Organisatie voor Wetenschappelijk Onderzoek (Netherlands Organisation for Scientific Research, NWO). T.J.H.V. acknowledges NWO-CW (Chemical Sciences) for a VICI grant. O.A.M. gratefully acknowledges the support of NVIDIA Corporation with the donation of the Titan V GPU used for this research.

REFERENCES

(1) Schwarzenbach, R. P.; Escher, B. I.; Fenner, K.; Hofstetter, T. B.; Johnson, C. A.; von Gunten, U.; Wehrli, B. The Challenge of Micropollutants in Aquatic Systems. *Science* **2006**, *313*, 1072−1077.

(2) Verliefde, A.; Cornelissen, E.; Amy, G.; Van der Bruggen, B.; van Dijk, H. Priority organic micropollutants in water sources in Flanders and the Netherlands and assessment of removal possibilities with nanofiltration. *Environ. Pollut.* **2007**, *146*, 281−289.

(3) Loos, R.; Locoro, G.; Comero, S.; Contini, S.; Schwesig, D.; Werres, F.; Balsaa, P.; Gans, O.; Weiss, S.; Blaha, L.; et al. Pan-European survey on the occurrence of selected polar organic

persistent pollutants in ground water. *Water Res.* **2010**, *44*, 4115−4126.
(4) Hut, R.; van de Giesen, N.; Houtman, C. J. Medicinal footprint of the population of the Rhine basin. *Environ. Res. Lett.* **2013**, *8*, No. 044057.
(5) Vulliet, E.; Cren-Olivé, C. Screening of pharmaceuticals and hormones at the regional scale, in surface and groundwaters intended to human consumption. *Environ. Pollut.* **2011**, *159*, 2929−2934.
(6) Luo, Y.; Guo, W.; Ngo, H. H.; Nghiem, L. D.; Hai, F. I.; Zhang, J.; Liang, S.; Wang, X. C. A review on the occurrence of micropollutants in the aquatic environment and their fate and removal during wastewater treatment. *Sci. Total Environ.* **2014**, *473-474*, 619−641.
(7) Yang, Y.; Ok, Y. S.; Kim, K.-H.; Kwon, E. E.; Tsang, Y. F. Occurrences and removal of pharmaceuticals and personal care products (PPCPs) in drinking water and water/sewage treatment plants: A review. *Sci. Total Environ.* **2017**, *596-597*, 303−320.
(8) Sousa, J. C. G.; Ribeiro, A. R.; Barbosa, M. O.; Pereira, M. F. R.; Silva, A. M. T. A review on environmental monitoring of water organic pollutants identified by EU guidelines. *J. Hazard. Mater.* **2018**, *344*, 146−162.
(9) Macova, M.; Toze, S.; Hodgers, L.; Mueller, J. F.; Bartkow, M.; Escher, B. I. Bioanalytical tools for the evaluation of organic micropollutants during sewage treatment, water recycling and drinking water generation. *Water Res.* **2011**, *45*, 4238−4247.
(10) Stamm, C.; Räsänen, K.; Burdon, F.; Altermatt, F.; Jokela, J.; Joss, A.; Ackermann, M.; Eggen, R. In *Large-Scale Ecology: Model Systems to Global Perspectives*; Dumbrell, A. J., Kordas, R. L., Woodward, G., Eds.; Advances in Ecological Research; Academic Press, 2016; Vol. 55; pp 183−223, DOI: 10.1016/bs.aecr.2016.07.002.
(11) Stackelberg, P. E.; Gibs, J.; Furlong, E. T.; Meyer, M. T.; Zaugg, S. D.; Lippincott, R. L. Efficiency of conventional drinking-water-treatment processes in removal of pharmaceuticals and other organic compounds. *Sci. Total Environ.* **2007**, *377*, 255−272.
(12) Loos, R.; Carvalho, R.; António, D. C.; Comero, S.; Locoro, G.; Tavazzi, S.; Paracchini, B.; Ghiani, M.; Lettieri, T.; Blaha, L.; et al. EU-wide monitoring survey on emerging polar organic contaminants in wastewater treatment plant effluents. *Water Res.* **2013**, *47*, 6475−6487.
(13) Margot, J.; Rossi, L.; Barry, D. A.; Holliger, C. A review of the fate of micropollutants in wastewater treatment plants. *Wiley Interdiscip. Rev.: Water* **2015**, *2*, 457−487.
(14) Oulton, R. L.; Kohn, T.; Cwiertny, D. M. Pharmaceuticals and personal care products in effluent matrices: A survey of transformation and removal during wastewater treatment and implications for wastewater management. *J. Environ. Monit.* **2010**, *12*, 1956−1978.
(15) Schwarzenbach, R. P.; Egli, T.; Hofstetter, T. B.; von Gunten, U.; Wehrli, B. Global Water Pollution and Human Health. *Annu. Rev. Environ. Resour.* **2010**, *35*, 109−136.
(16) Crini, G.; Lichtfouse, E. Advantages and disadvantages of techniques used for wastewater treatment. *Environ. Chem. Lett.* **2019**, *17*, 145−155.
(17) Luan, M.; Jing, G.; Xu, X.; Hou, B.; Wang, Y.; Meng, D. A review: Wet oxidation and catalytic wet oxidation of industrial wastewater. *Recent Pat. Chem. Eng.* **2013**, *6*, 79−86.
(18) Shannon, M. A.; Bohn, P. W.; Elimelech, M.; Georgiadis, J. G.; Mariñas, B. J.; Mayes, A. M. Science and technology for water purification in the coming decades. *Nature* **2008**, *452*, 301−310.
(19) Gaya, U. I.; Abdullah, A. H. Heterogeneous photocatalytic degradation of organic contaminants over titanium dioxide: A review of fundamentals, progress and problems. *J. Photochem. Photobiol., C* **2008**, *9*, 1−12.
(20) Cath, T.; Childress, A.; Elimelech, M. Forward osmosis: Principles, applications, and recent developments. *J. Membr. Sci.* **2006**, *281*, 70−87.
(21) Sun, P.; Meng, T.; Wang, Z.; Zhang, R.; Yao, H.; Yang, Y.; Zhao, L. Degradation of Organic Micropollutants in UV/NH_2Cl Advanced Oxidation Process. *Environ. Sci. Technol.* **2019**, *53*, 9024−9033.
(22) Ali, I.; Gupta, V. K. Advances in water treatment by adsorption technology. *Nat. Protoc.* **2006**, *1*, 2661−2667.
(23) Chen, D.; Wang, L.; Ma, Y.; Yang, W. Super-adsorbent material based on functional polymer particles with a multilevel porous structure. *NPG Asia Mater.* **2016**, *8*, e301.
(24) Trewin, A.; Cooper, A. I. Porous Organic Polymers: Distinction from Disorder? *Angew. Chem., Int. Ed.* **2010**, *49*, 1533−1535.
(25) Thomas, A. Functional Materials: From Hard to Soft Porous Frameworks. *Angew. Chem., Int. Ed.* **2010**, *49*, 8328−8344.
(26) Zhang, W.; Aguila, B.; Ma, S. Retraction: Potential applications of functional porous organic polymer materials. *J. Mater. Chem. A* **2017**, *5*, 18896−18896.
(27) Tan, L.; Tan, B. Hypercrosslinked porous polymer materials: design, synthesis, and applications. *Chem. Soc. Rev.* **2017**, *46*, 3322−3356.
(28) Sawicki, R.; Mercier, L. Evaluation of Mesoporous Cyclodextrin-Silica Nanocomposites for the Removal of Pesticides from Aqueous Media. *Environ. Sci. Technol.* **2006**, *40*, 1978−1983.
(29) Zhao, F.; Repo, E.; Yin, D.; Meng, Y.; Jafari, S.; Sillanpää, M. EDTA-Cross-Linked β-Cyclodextrin: An Environmentally Friendly Bifunctional Adsorbent for Simultaneous Adsorption of Metals and Cationic Dyes. *Environ. Sci. Technol.* **2015**, *49*, 10570−10580.
(30) Biwer, A.; Antranikian, G.; Heinzle, E. Enzymatic production of cyclodextrins. *Appl. Microbiol. Biotechnol.* **2002**, *59*, 609−617.
(31) Crini, G. Review: A History of Cyclodextrins. *Chem. Rev.* **2014**, *114*, 10940−10975.
(32) Connors, K. A. The Stability of Cyclodextrin Complexes in Solution. *Chem. Rev.* **1997**, *97*, 1325−1358.
(33) Marques, H. M. C. A review on cyclodextrin encapsulation of essential oils and volatiles. *Flavour Fragrance J.* **2010**, *25*, 313−326.
(34) Balabai, N.; Linton, B.; Napper, A.; Priyadarshy, S.; Sukharevsky, A. P.; Waldeck, D. H. Orientational Dynamics of β-Cyclodextrin Inclusion Complexes. *J. Phys. Chem. B* **1998**, *102*, 9617−9624.
(35) Carrazana, J.; Jover, A.; Meijide, F.; Soto, V. H.; Vázquez Tato, J. Complexation of Adamantyl Compounds by β-Cyclodextrin and Monoaminoderivatives. *J. Phys. Chem. B* **2005**, *109*, 9719−9726.
(36) Hollas, M.; Chung, M.-A.; Adams, J. Complexation of Pyrene by Poly(allylamine) with Pendant β-Cyclodextrin Side Groups. *J. Phys. Chem. B* **1998**, *102*, 2947−2953.
(37) Naughton, H. R.; Abelt, C. J. Local Solvent Acidities in β-Cyclodextrin Complexes with PRODAN Derivatives. *J. Phys. Chem. B* **2013**, *117*, 3323−3327.
(38) Alzate-Sánchez, D. M.; Ling, Y.; Li, C.; Frank, B. P.; Bleher, R.; Fairbrother, D. H.; Helbling, D. E.; Dichtel, W. R. β-Cyclodextrin Polymers on Microcrystalline Cellulose as a Granular Media for Organic Micropollutant Removal from Water. *ACS Appl. Mater. Interfaces* **2019**, *11*, 8089−8096.
(39) Alsbaiee, A.; Smith, B. J.; Xiao, L.; Ling, Y.; Helbling, D. E.; Dichtel, W. R. Rapid removal of organic micropollutants from water by a porous β-cyclodextrin polymer. *Nature* **2016**, *529*, 190−194.
(40) Wang, J.; Wang, X.; Zhang, X. Cyclic molecule aerogels: a robust cyclodextrin monolith with hierarchically porous structures for removal of micropollutants from water. *J. Mater. Chem. A* **2017**, *5*, 4308−4313.
(41) Ling, Y.; Klemes, M. J.; Xiao, L.; Alsbaiee, A.; Dichtel, W. R.; Helbling, D. E. Benchmarking Micropollutant Removal by Activated Carbon and Porous β-Cyclodextrin Polymers under Environmentally Relevant Scenarios. *Environ. Sci. Technol.* **2017**, *51*, 7590−7598.
(42) Wang, Z.; Zhang, P.; Hu, F.; Zhao, Y.; Zhu, L. A crosslinked β-cyclodextrin polymer used for rapid removal of a broad-spectrum of organic micropollutants from water. *Carbohydr. Polym.* **2017**, *177*, 224−231.
(43) Morin-Crini, N.; Winterton, P.; Fourmentin, S.; Wilson, L. D.; Fenyvesi, É.; Crini, G. Water-insoluble β-cyclodextrin−epichlorohydrin polymers for removal of pollutants from aqueous solutions by

sorption processes using batch studies: A review of inclusion mechanisms. *Prog. Polym. Sci.* **2018**, *78*, 1−23.
(44) Geitner, N. K.; Zhao, W.; Ding, F.; Chen, W.; Wiesner, M. R. Mechanistic Insights from Discrete Molecular Dynamics Simulations of Pesticide−Nanoparticle Interactions. *Environ. Sci. Technol.* **2017**, *51*, 8396−8404.
(45) Lan, T.; Liao, J.; Yang, Y.; Chai, Z.; Liu, N.; Wang, D. Competition/Cooperation between Humic Acid and Graphene Oxide in Uranyl Adsorption Implicated by Molecular Dynamics Simulations. *Environ. Sci. Technol.* **2019**, *53*, 5102−5110.
(46) Sellner, B.; Zifferer, G.; Kornherr, A.; Krois, D.; Brinker, U. H. Molecular Dynamics Simulations of β-Cyclodextrin-Aziadamantane Complexes in Water. *J. Phys. Chem. B* **2008**, *112*, 710−714.
(47) Sun, H. COMPASS: An ab-initio Force-Field Optimized for Condensed-Phase Applications Overview with Details on Alkane and Benzene Compounds. *J. Phys. Chem. B* **1998**, *102*, 7338−7364.
(48) Mayo, S. L.; Olafson, B. D.; Goddard, W. A. DREIDING: a generic force field for molecular simulations. *J. Phys. Chem.* **1990**, *94*, 8897−8909.
(49) Henriksen, N. M.; Gilson, M. K. Evaluating Force Field Performance in Thermodynamic Calculations of Cyclodextrin Host−Guest Binding: Water Models, Partial Charges, and Host Force Field Parameters. *J. Chem. Theory Comput.* **2017**, *13*, 4253−4269.
(50) Tang, Z.; Chang, C.-E. A. Binding Thermodynamics and Kinetics Calculations Using Chemical Host and Guest: A Comprehensive Picture of Molecular Recognition. *J. Chem. Theory Comput.* **2017**, *14*, 303−318.
(51) Yin, J.; Henriksen, N. M.; Muddana, H. S.; Gilson, M. K. Bind3P: Optimization of a Water Model Based on Host−Guest Binding Data. *J. Chem. Theory Comput.* **2018**, *14*, 3621−3632.
(52) Zhu, X.; Wu, G.; Chen, D. Molecular dynamics simulation of cyclodextrin aggregation and extraction of Anthracene from non-aqueous liquid phase. *J. Hazard. Mater.* **2016**, *320*, 169−175.
(53) Zhang, H.; Ge, C.; van der Spoel, D.; Feng, W.; Tan, T. Insight into the Structural Deformations of Beta-Cyclodextrin Caused by Alcohol Cosolvents and Guest Molecules. *J. Phys. Chem. B* **2012**, *116*, 3880−3889.
(54) Zhang, H.; Tan, T.; Hetényi, C.; Lv, Y.; van der Spoel, D. Cooperative Binding of Cyclodextrin Dimers to Isoflavone Analogues Elucidated by Free Energy Calculations. *J. Phys. Chem. C* **2014**, *118*, 7163−7173.
(55) Zhang, H.; Tan, T.; Hetényi, C.; van der Spoel, D. Quantification of Solvent Contribution to the Stability of Non-covalent Complexes. *J. Chem. Theory Comput.* **2013**, *9*, 4542−4551.
(56) Piñeiro, Á.; Banquy, X.; Pérez-Casas, S.; Tovar, E.; García, A.; Villa, A.; Amigo, A.; Mark, A. E.; Costas, M. On the Characterization of Host-Guest Complexes: Surface Tension, Calorimetry, and Molecular Dynamics of Cyclodextrins with a Non-ionic Surfactant. *J. Phys. Chem. B* **2007**, *111*, 4383−4392.
(57) Semino, R.; Rodríguez, J. Molecular Dynamics Study of Ionic Liquids Complexation within β-Cyclodextrins. *J. Phys. Chem. B* **2015**, *119*, 4865−4872.
(58) Sancho, M. I.; Andujar, S.; Porasso, R. D.; Enriz, R. D. Theoretical and Experimental Study of Inclusion Complexes of β-Cyclodextrins with Chalcone and 2,4-Dihydroxychalcone. *J. Phys. Chem. B* **2016**, *120*, 3000−3011.
(59) Oda, M.; Kuroda, M. Molecular dynamics simulations of inclusion complexation of glycyrrhizic acid and cyclodextrins (1:1) in water. *J. Inclusion Phenom. Macrocyclic Chem.* **2016**, *85*, 271−279.
(60) Felton, L. A.; Popescu, C.; Wiley, C.; Esposito, E. X.; Lefevre, P.; Hopfinger, A. J. Experimental and Computational Studies of Physicochemical Properties Influence NSAIDCyclodextrin Complexation. *AAPS PharmSciTech* **2014**, *15*, 872−881.
(61) Guzzo, T.; Mandaliti, W.; Nepravishta, R.; Aramini, A.; Bodo, E.; Daidone, I.; Allegretti, M.; Topai, A.; Paci, M. Conformational Change in the Mechanism of Inclusion of Ketoprofen in β-Cyclodextrin: NMR Spectroscopy, Ab Initio Calculations, Molecular Dynamics Simulations, and Photoreactivity. *J. Phys. Chem. B* **2016**, *120*, 10668−10678.
(62) Škvára, J.; Nezbeda, I. Molecular dynamics study of racemic mixtures: Solutions of ibuprofen and β-cyclodextrin in methanol. *J. Mol. Liq.* **2018**, *265*, 791−796.
(63) Wang, R.; Zhou, H.; Siu, S. W. I.; Gan, Y.; Wang, Y.; Ouyang, D. Comparison of Three Molecular Simulation Approaches for Cyclodextrin-Ibuprofen Complexation. *J. Nanomater.* **2015**, *2015*, 193049.
(64) Pinto, L. M. A.; de Jesus, M. B.; de Paula, E.; Lino, A. C. S.; Alderete, J. B.; Duarte, H. A.; Takahata, Y. Elucidation of inclusion compounds between β-cyclodextrin/local anaesthetics structure: a theoretical and experimental study using differential scanning calorimetry and molecular mechanics. *J. Mol. Struct.: THEOCHEM* **2004**, *678*, 63−66.
(65) European Comission Development of the first Watch List under the Environmental Quality Standards Directive. Available at http://publications.jrc.ec.europa.eu/repository/bitstream/JRC95018/lbna27142enn.pdf (2019.09.22).
(66) European Comission Directive of the European Parliament ad of the Council amending Directives 2000/60/EC and 2008/105/EC as regards priority substances in the field of water policy. Available at https://eur-lex.europa.eu/legal-content/EN/TXT/PDF/?uri=CELEX:52011PC0876&from=EN (2019.09.22).
(67) Huff, J. Long-term toxicology and carcinogenicity of 2,4,6-trichlorophenol. *Chemosphere* **2012**, *89*, 521−525.
(68) Henriksen, N. M.; Fenley, A. T.; Gilson, M. K. Computational Calorimetry: HighPrecision Calculation of Host−Guest Binding Thermodynamics. *J. Chem. Theory Comput.* **2015**, *11*, 4377−4394.
(69) Abraham, M. J.; Murtola, T.; Schulz, R.; Páll, S.; Smith, J. C.; Hess, B.; Lindahl, E. GROMACS: High performance molecular simulations through multi-level parallelism from laptops to supercomputers. *SoftwareX* **2015**, *1-2*, 19−25.
(70) Cézard, C.; Trivelli, X.; Aubry, F.; Djedaïni-Pilard, F.; Dupradeau, F.-Y. Molecular dynamics studies of native and substituted cyclodextrins in different media: 1. Charge derivation and force field performances. *Phys. Chem. Chem. Phys.* **2011**, *13*, 15103−15121.
(71) Wang, J.; Wolf, R. M.; Caldwell, J. W.; Kollman, P. A.; Case, D. A. Development and testing of a general Amber force field. *J. Comput. Chem.* **2004**, *25*, 1157−1174.
(72) Joung, I. S.; Cheatham, T. E., III Determination of Alkali and Halide Monovalent Ion Parameters for Use in Explicitly Solvated Biomolecular Simulations. *J. Phys. Chem. B* **2008**, *112*, 9020−9041.
(73) Jorgensen, W. L.; Chandrasekhar, J.; Madura, J. D.; Impey, R. W.; Klein, M. L. Comparison of simple potential functions for simulating liquid water. *J. Chem. Phys.* **1983**, *79*, 926−935.
(74) Dupradeau, F.-Y.; Pigache, A.; Zaffran, T.; Savineau, C.; Lelong, R.; Grivel, N.; Lelong, D.; Rosanski, W.; Cieplak, P. The R.E.D. tools: advances in RESP and ESP charge derivation and force field library building. *Phys. Chem. Chem. Phys.* **2010**, *12*, 7821−7839.
(75) Frisch, M. J.; Trucks, G. W.; Schlegel, H. B.; Scuseria, G. E.; Robb, M. A.; Cheeseman, J. R.; Montgomery, J. A., Jr.; Vreven, T.; Kudin, K. N.; Burant, J. C. et al. *Gaussian 09*, Revision B.01. Gaussian, Inc.: Wallingford, CT, 2016.
(76) Darden, T.; York, D.; Pedersen, L. Particle mesh Ewald: An Nlog(N) method for Ewald sums in large systems. *J. Chem. Phys.* **1993**, *98*, 10089−10092.
(77) Goga, N.; Rzepiela, A. J.; de Vries, A. H.; Marrink, S. J.; Berendsen, H. J. C. Efficient algorithms for Langevin and DPD dynamics. *J. Chem. Theory Comput.* **2012**, *8*, 3637−3649.
(78) Berendsen, H. J. C.; Postma, J. P. M.; van Gunsteren, W. F.; DiNola, A.; Haak, J. R. Molecular dynamics with coupling to an external bath. *J. Chem. Phys.* **1984**, *81*, 3684−3690.
(79) Fenley, A. T.; Henriksen, N. M.; Muddana, H. S.; Gilson, M. K. Bridging Calorimetry and Simulation through Precise Calculations of Cucurbituril−Guest Binding Enthalpies. *J. Chem. Theory Comput.* **2014**, *10*, 4069−4078.
(80) Flyvbjerg, H.; Petersen, H. G. Error estimates on averages of correlated data. *J. Chem. Phys.* **1989**, *91*, 461−466.

https://dx.doi.org/10.1021/acs.jpcb.9b10122
J. Phys. Chem. B 2020, 124, 1218−1228

(81) Del Valle, E. M. M. Cyclodextrins and their uses: a review. *Process Biochem.* **2004**, *39*, 1033−1046.
(82) Zhou, H.-X.; Gilson, M. K. Theory of Free Energy and Entropy in Noncovalent Binding. *Chem. Rev.* **2009**, *109*, 4092−4107.
(83) Waters, L. J.; Bedford, S.; Parkes, G. M. B.; Mitchell, J. C. Influence of lipophilicity on drug−cyclodextrin interactions: A calorimetric study. *Thermochim. Acta* **2010**, *511*, 102−106.
(84) Rozou, S.; Michaleas, S.; Antoniadou-Vyza, E. Study of structural features and thermodynamic parameters, determining the chromatographic behaviour of drug-cyclodextrin complexes. *J. Chromatogr. A* **2005**, *1087*, 86−94.
(85) Mochida, K.; Kagita, A.; Matsui, Y.; Date, Y. Effects of Inorganic Salts on the Dissociation of a Complex of β-Cyclodextrin with an Azo Dye in an Aqueous Solution. *Bull. Chem. Soc. Jpn.* **1973**, *46*, 3703−3707.
(86) Terekhova, I. V.; Chibunova, E. S.; Kumeev, R. S.; Alper, G. A. Cyclodextrin−benzoic acid binding in salt solutions: Effects of biologically relevant anions. *Carbohydr. Polym.* **2014**, *110*, 472−479.
(87) Mobley, D. L.; Gilson, M. K. Predicting Binding Free Energies: Frontiers and Benchmarks. *Annu. Rev. Biophys.* **2017**, *46*, 531−558.
(88) Vidal, R. B. P.; Ibañez, G. A.; Escandar, G. M. Spectrofluorimetric study of phenolic endocrine disruptors in cyclodextrin media. *RSC Adv.* **2015**, *5*, 20914−20923.
(89) Mironov, G. G.; Logie, J.; Okhonin, V.; Renaud, J. B.; Mayer, P. M.; Berezovski, M. V. Comparative Study of Three Methods for Affinity Measurements: Capillary Electrophoresis Coupled with UV Detection and Mass Spectrometry, and Direct Infusion Mass Spectrometry. *J. Am. Soc. Mass Spectrom.* **2012**, *23*, 1232−1240.
(90) Chelli, S.; Majdoub, M.; Jouini, M.; Aeiyach, S.; Maurel, F.; Chane-Ching, K. I.; Lacaze, P.-C. Host−guest complexes of phenol derivatives with β-cyclodextrin: an experimental and theoretical investigation. *J. Phys. Org. Chem.* **2007**, *20*, 30−43.
(91) di Cagno, M.; Stein, P. C.; Skalko-Basnet, N.; Brandl, M.; Bauer-Brandl, A. Solubilization of ibuprofen with β-cyclodextrin derivatives: Energetic and structural studies. *J. Pharm. Biomed. Anal.* **2011**, *55*, 446−451.
(92) Chadha, R.; Kashid, N.; Kumar, A.; Jain, D. V. S. Calorimetric studies of diclofenac sodium in aqueous solution of cyclodextrin and water-ethanol mixtures. *J. Pharm. Pharmacol.* **2002**, *54*, 481−486.
(93) Hanna, K.; de Brauer, C.; Germain, P. Solubilization of the neutral and charged forms of 2,4,6-trichlorophenol by β-cyclodextrin, methyl-β-cyclodextrin and hydroxypropyl-β-cyclodextrin in water. *J. Hazard. Mater.* **2003**, *100*, 109−116.
(94) Brown, G. R.; Caira, M. R.; Nassimbeni, L. R.; Oudtshoorn, B. Inclusion of ibuprofen by heptakis(2,3,6-tri-O-methyl)-β-cyclodextrin: An X-ray diffraction and thermal analysis study. *J. Inclusion Phenom. Mol. Recognit. Chem.* **1996**, *26*, 281−294.
(95) Braga, S. S.; Gonçalves, I. S.; Herdtweck, E.; Teixeira-Dias, J. J. C. Solid state inclusion compound of S-ibuprofen in β-cyclodextrin: structure and characterisation. *New J. Chem.* **2003**, *27*, 597−601.

https://dx.doi.org/10.1021/acs.jpcb.9b10122
J. Phys. Chem. B 2020, 124, 1218−1228